

Mechanism of the pseudogap and possible 61 meV pseudogap at 300 K for underdoped $\text{Bi}_2\text{Sr}_2\text{CaCu}_2\text{O}_{8+\delta}$

Fu-sui Liu*

Physics Department, Beijing University, Beijing 100871, China

Wan-fang Chen

*CCAST (World Laboratory), P. O. Box 8730, Beijing 100080, China**and University of Science and Technology of Staffs and Workers of Academy of Science of China, Beijing 100080, China*

(Received 17 November 1997; revised manuscript received 30 March 1998)

Based on the temperature dependence of two-local-spin-mediated interaction for $\text{Br}_2\text{Sr}_2\text{CaCu}_2\text{O}_{8+\delta}$ (B2212), this paper explains the fourteen features of the pseudogap (PG) in underdoped B2212, and makes three predictions. The most unusual prediction is the existence of a 61 meV PG at 300 K in the range of $T_c = 0$ for underdoped B2212. [S0163-1829(98)10237-0]

I. INTRODUCTION

Recently a number of experiments on the underdoped high- T_c cuprates have revealed the opening of a pseudogap (PG) in the excitation spectrum at $T_c < T < T^*$.¹⁻²⁰ T^* is well above the superconductive transition temperature T_c . This paper investigates the following fourteen observed features of the PG. First, all the materials with both single and double CuO_2 planes in one unit cell have PG.^{1,5,10} Second, the lower the x , the higher the T^* for $x > 0.056$.^{2,9} The x is the number of $\text{O}_{p\sigma}$ holes in a CuO_2 cell. Third, the shift of T^* with pressure, p , is $dT^*/dp < 0$.¹¹ Fourth, the dc resistivity at $T < T^*$ goes down more quickly than the linear temperature relation.⁹ Fifth, that the T^* can be determined by electronic tunneling,⁷ resistivity,⁹ and photoemission^{2,3} shows that PG might not be in the single spin channel. Sixth, there is no energy jump of the gap to PG at T_c .² Seventh, the dependence of PG on temperature might be very complex. However, considering the large error bars in Ref. 2, the data cannot support any kind of theoretical curves. Eighth, the higher the x , the lower the E_g for $x \geq 0.08$, decreasing to zero at about $x = 0.19$.⁵ E_g is PG at T_c . Ninth, $2(\text{gap at } 0 \text{ K})/T_c$ may be much larger than BCS value 3.54. Tenth, PG decreases with increasing T_c at $44 \text{ K} \leq T_c \leq 93 \text{ K}$.^{4,9,17} Eleventh, PG is of anisotropy, i.e., the node of PG is at the direction 45° rotating from the Cu-O bond,²⁻⁴ and the maximum PG direction is controversial in experiments. It might be at about 10° from the Cu-O bond,² or just at the Cu-O bond direction.^{3,4} It is very interesting to note that the observed difference of PG maximum direction also exists in measurements for the gap of the overdoped high- T_c cuprates.²¹⁻²³ Twelfth, absence of isotope effect in PG in $\text{YBa}_2\text{Cu}_4\text{O}_8$.¹⁸ Thirteenth, some high- T_c cuprates such as $\text{LaBa}_2\text{Cu}_3\text{O}_y$ have PG for all doped levels.¹⁹ Fourteenth, STM experiment shows that some local regions in the CuO_2 plane of B2212 have unusual properties.²⁰ Due to the fact that the data in Ref. 20 are not clearly given, we state the experimental results in Ref. 20 as follows. In certain chosen $0.15 \mu\text{m}$ range in the CuO_2 plane of 83 K T_c underdoped B2212 ($x = 0.125$) the gap is nearly temperature independent

up to T_c , and PG is about 70 meV at 293 K.²⁰ For 74.3 K T_c overdoped B2212 ($x = 0.209$) PG is not zero.²⁰

Many theoretical explanations for PG have been proposed.²⁴⁻³³ Some authors²⁴⁻²⁷ believe that the spinons form singlet pairs well above T_c , with superconductivity setting in only when there is the holon Bose condensation at T_c . Some authors attribute PG to the ordinary band gap,²⁸ however, the fourth feature seems to not qualitatively support it. Using an assumed local pairing potential, the quasipin Monte Carlo simulation shows that the uncorrelated bound hole pair can be produced above T_c ;²⁹ however, its relation between T^* and x is opposite to the second feature. According to the SO(5) symmetry theory of superconductivity and antiferromagnetism (AF), T^* is identified with the temperature at which the superspin amplitude forms.³⁰ However, whether or not the t - J model, or the single band Hubbard model, from which the approximate SO(5) symmetry is derived, can correctly describe the high- T_c superconductivity has not yet been completely determined.³⁴ The phenomenological theories proposed in Refs. 31-33, completely independent of any superconductive mechanisms, conclude that there are Cooper pairs without, and with long-range phase coherence (LRPC) between T^* and T_c , and below T_c , respectively. However, Ref. 25 thinks that the superconductive state is destroyed by thermal excitation of just the low lying quasiparticles, and believes its scenario is better than the phase coherence scenario in Refs. 31-33.

Based on detailed consideration of the temperature dependence for TLSMI in Refs. 35-44, and numerical solution of BCS gap equation, this paper explains all the fourteen features, and some explanations are even quantitative. Our theory supports the theory in Refs. 31-33, and concludes that the gaps without and with LRPC are the solutions in different temperature ranges of the same BCS gap equation. This paper gives three predictions. First, the temperature dependence of the gap at $0 < T < T^*$ is of three types, and two of them deviate from BCS type seriously. Second, the maximum value of the gap at $0 < T < T^*$ for B2212 is along the direction about 10° rotating from the Cu-O bond instead of 0° in spin fluctuation theory.^{34,45} Third, there might be a

weak Meissner effect in the range of $T_c < T < T^*$. The most unusual property in the first prediction is the existence of a 61 meV PG at 300 K for the B2212 sample with $T_c = 0$ and $x = 0.025$.

II. TWO-LOCAL-SPIN-MEDIATED INTERACTION MECHANISM

Using the extended Abrikosov's pseudofermion method in the Appendix and Refs. 35–37, Liu showed that there is an attractive two-nearest-Cu⁺⁺-local-spin-mediated interaction (TLSMI) between two $O_{p\sigma}$ holes with $\mathbf{k}\uparrow$ and $-\mathbf{k}\downarrow$ in the AF CuO_2 plane, and the high- T_c is caused by TLSMI.^{38–44} For readers' convenience we write down the major formulas in Refs. 38–44. The formula of TLSMI has been given in Refs. 40 and 44, and is quoted as follows:

$$U_{\mathbf{k}\mathbf{k}'} = -A(T)F_{\mathbf{k}\mathbf{k}'}, \quad (1)$$

$$A(T) = \frac{0.5JJ_K^2(1+C)N''/N'w(J/T)}{T^2 + 8JJ_K^2 \sum_{\mathbf{k}\mathbf{p}} g(\mathbf{k}, \mathbf{p}) / \{1 + 32\pi^2 J_K^2 [N(E_F)]^2 \overline{h(\mathbf{q})}\}}, \quad (2)$$

$$g(\mathbf{k}, \mathbf{p}) = \left(\frac{1}{2N_{\text{Cu}}} \right)^2 \frac{f[\varepsilon(\mathbf{k}) - E_F]F_1(\mathbf{k})F_1(\mathbf{p})F_5(\mathbf{k})F_5(\mathbf{p})}{\varepsilon(\mathbf{k}) - \varepsilon(\mathbf{p})}, \quad (3)$$

$$h(\mathbf{k}) = [\cos(k_x a/2)\cos(k_y a/2)]^4, \quad (4)$$

$$F_{\mathbf{k}\mathbf{k}'} = \sum_{i=1}^4 F_i(\mathbf{k})F_i(\mathbf{k}')F_5(\mathbf{k})F_5(\mathbf{k}'), \quad (5)$$

$$F_1(\mathbf{k}) = \cos(k_x a)\cos(k_y a), \quad (6)$$

$$F_2(\mathbf{k}) = \sin(k_x a)\sin(k_y a), \quad (7)$$

$$F_3(\mathbf{k}) = \sin(k_x a)\cos(k_y a), \quad (8)$$

$$F_4(\mathbf{k}) = \cos(k_x a)\sin(k_y a), \quad (9)$$

$$F_5(\mathbf{k}) = \cos^2(k_x a)\cos^2(k_y a), \quad (10)$$

where a is the nearest distance between two oxygen atoms in the CuO_2 plane, N_{Cu} is the number of Cu^{++} in the CuO_2 plane, \mathbf{k} , \mathbf{p} , and \mathbf{q} are wave vector in the Brillouin zone of the oxygen lattice, $f(x)$ is Fermi distribution, $\varepsilon(\mathbf{k})$ energy of $O_{p\sigma}$ holes, E_F Fermi energy, $N(E_F)$ density of states, C weak tunneling coupling between two CuO_2 planes if the cuprates have two CuO_2 planes in a unit cell, J coupling constant between two nearest neighbor Cu^{++} s, J_K coupling constant between local Cu^{++} spin and mobile $O_{p\sigma}$ hole spin. The bar represents the average on a Fermi surface. N'' and N' are the number of Cu^{++} pairs in the nearest neighbor and the total number of Cu^{++} in a cluster being of AF short range order, ξ , respectively. The curves of N''/N' vs ξ have been given in Refs. 40 and 44. $w(J/T) = 1 + f_1/f_2$ is the transformation factor in Eq. (A41) of the Appendix.

The BCS equation of the gap function is

$$\Delta'(T, \mathbf{k}) = - \sum_{\mathbf{k}'} \frac{U_{\mathbf{k}\mathbf{k}'} \Delta'(T, \mathbf{k}')}{2m(T, \mathbf{k}')} \tanh \frac{m(T, \mathbf{k}')}{2T}, \quad (11)$$

$$m(T, \mathbf{k}) = \sqrt{[\varepsilon(\mathbf{k}) - E_F]^2 + |\Delta'(T, \mathbf{k})|^2}. \quad (12)$$

The solution of Eq. (11) is a true gap with an undetermined phase. Therefore the temperature determined by the zero gap condition is, generally speaking, T^* , which is different from T_c . If $T \leq T_c$, the gap is of LRPC because the system is in a superconductive state. If $T^* > T > T_c$, then the gap is not of LRPC. As we know, the superconductivity in the high- T_c cuprates needs LRPC besides the gap. The non-zero gap condition is only a necessary condition. Therefore, the reasonable relation between T^* and T_c is $T^* \geq T_c$. The main solution of Eq. (11) has already been given in Refs. 40 and 44, and is quoted as follows:

$$\Delta'(T, \mathbf{k}) = \Delta(T)F_2(\mathbf{k})F_5(\mathbf{k}), \quad (13)$$

In the 45°-rotating coordinate system corresponding to the Cu-O bond, $F_2(\mathbf{k}') = [\cos(k'_x a') - \cos(k'_y a')]/2$, i.e., the simple d -wave in many high- T_c mechanisms.^{34,45,30} The a' is the nearest distance between two Cu^{++} s. Equation (13) is called a composite d -wave gap because of the extra $F_5(\mathbf{k})$ factor. Although all the formulas from Eqs. (1) to (13) have been given in Refs. 38–44, our previous calculations ignored two important temperature dependences, i.e., we take $w(J/T) = 1 + f_1/f_2 = 1$ in Eq. (2), and $T = 0$ K for the Fermi distribution in Eq. (3), and we therefore have not yet obtained PG from the solution of the BCS gap equation in Refs. 38–44. Considering the temperature dependence of $w(J/T)$ and the Fermi distribution, this paper not only shows the existence of PG but also explains all the fourteen features of PG. The most unusual prediction in this paper is the existence of 61 meV PG at 300 K for underdoped B2212 with $T_c = 0$.

III. THE VALUES OF PARAMETERS

The values of parameters appearing in Eq. (11) can be determined by experiments basically. The observed Fermi surface of B2212 with $x = 0.2$ is $-3.12[\cos(k'_x a') - \cos(k'_y a')] = E_F = -0.28$ eV.⁴⁶ Because of using the B2212 Fermi surface, the quantitative comparison of our theory with experiments for materials other than B2212 has only reference value. The dependence of E_F on x can be determined by the rigid band consideration. J is a function of x , $J(x) = J(0)(1 - 1.77x)$ for $x < 0.28$.⁴⁷ $J(0) = 0.12$ eV at $x = 0$.⁴⁸ $\xi = a'/\sqrt{x}$ if $x < 0.15$.⁴⁹ $\xi < a'/\sqrt{x}$ if $x > 0.15$.⁵⁰ $C = 0.1$. $J_K = t^2/[1/(U_d - \varepsilon_p + \varepsilon_d - 2V_o) + 1/(\varepsilon_p - \varepsilon_d + U_p)]$.^{51–54} $\varepsilon_p - \varepsilon_d = 1.6$ eV, $U_d = 12$ eV, $U_p = 8.7$ eV, $V_o = 3.6$ eV, and $t = 1.4$ eV,⁵⁵ and therefore $J_K = 0.78$ eV. Many authors use the empirical formula, $T_c = T_{c, \text{max}}[1 - 82.6(x - 0.16)^2]$, to estimate experimental x from observed T_c ,⁵ and this paper will do so as well.

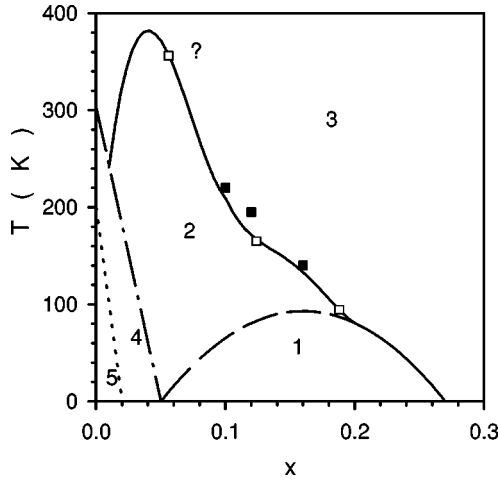


FIG. 1. Phase diagram of B2212. The solid line is our theoretical curve of T^* vs x . The dashed line is given by $T_c = 93[1 - 82.6(x - 0.16)^2]$. The above two curves coincide between $x = 0.20$ and 0.27 . The data of T^* vs x are from Ref. 9 (solid square) and Ref. 2 (square). Because T^* at $x = 0.056$ given in Ref. 2 is only larger than 301 K, we put a question mark for the datum. All the data are for B2212. The states in range 1, 3, and 5 are superconductive, normal, and insulating with long-range AF order (Ref. 56), respectively. There are Cooper pairs without long-range phase coherence in the range 2. The range 4 is a special insulating state, in which a Coulomb gap appears to add or to subtract a Cooper pair from a given domain (Ref. 33).

IV. EXPLANATIONS FOR THE FOURTEEN FEATURES OF PG

Based on a great quantity of numerical calculations for Eq. (11), many features among the fourteen features can be explained by only one word. Let us explain the fourteen features of PG one by one. The difference between the single and the double CuO_2 planes in one unit cell is only in $C = 0$ or 0.1 in Eq. (2), thus both the single and the double cases should have PG. Figure 1 shows that the lower the x , the higher the T^* for $x > 0.056$. Because the applied pressure p causes extra holes to be pushed into the CuO_2 plane,¹¹ i.e., $dx/dp > 0$, we have $dT^*/dp < 0$ for $x > 0.05$ from Fig. 1. Although Cooper pairs between T^* and T_c lose LRPC, and therefore the global superconductive state, they can still have short-range phase coherence, and therefore there is supercon-

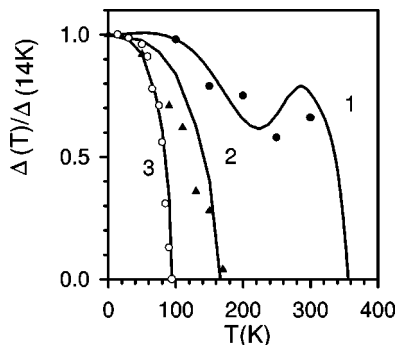


FIG. 2. Dependence of PG and the gap on T for B2212. $\Delta(T)$ is the maximum value of our composite d -wave PG and the gap. The curves 1, 2, and 3 are for $x = 0.056$, 0.125 , and 0.188 , respectively. The corresponding data are from Ref. 2.

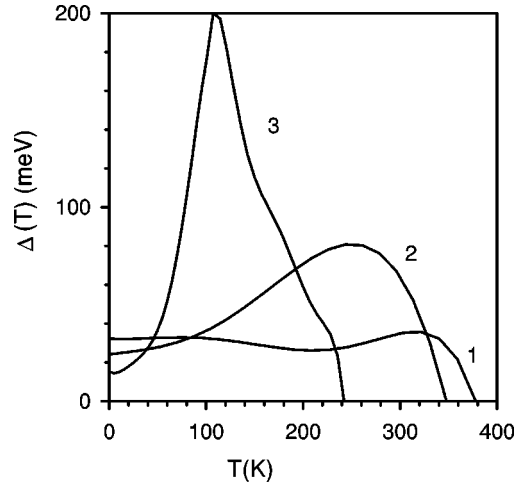


FIG. 3. Dependence of PG on T for B2212. The curves 1, 2, and 3 are for $x = 0.05$, 0.025 , and 0.01 , respectively.

ductive state in many small regions, which leads to the decrease of dc resistivity. It is obvious that there is no separation of charge and spin in our theory; therefore PG is not in single spin channel. The absolute values of the gap and PG at T_c are identical because the gap and PG all are the uniform solution with different phases of Eq. (11); therefore there is no energy jump of the gap into PG at T_c . Our theory can give complex temperature relation of PG shown in Figs. 2 and 3 because our theory has three new temperature factors, Fermi distribution, $w(J/T)$, and T^2 in Eq. (2), which do not exist in the ordinary BCS theory. Figure 4 shows that the higher the x , the lower the E_g for $x > 0.075$, decreasing to zero at $x = 0.2$. Figure 5 shows that $2\Delta(0 \text{ K})/T_c = 80$ at $x = 0.056$, which is much larger than the ordinary BCS 3.54. Note that the values of $2\Delta(0 \text{ K})/T^*$ is still a little larger than 3.54. Figure 6 shows that the gap at 0 K decreases with increasing x , or T_c , at $0.08 \leq x \leq 0.16$, or $43.8 \text{ K} \leq T_c \leq 93 \text{ K}$. The data in Fig. 7 indicate that PG is of anisotropy, and, especially, PG has a maximum at about 10° instead of

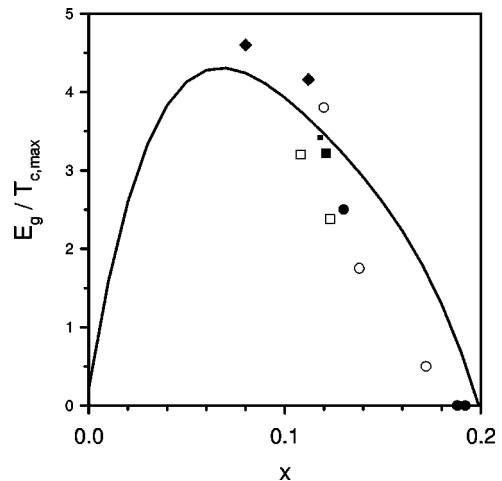


FIG. 4. Dependence of PG at T_c , i.e., E_g , on x . The data are from Ref. 5. The solid circle is for B2212, the circle $\text{YBa}_2\text{Cu}_3\text{O}_{7-\delta}$, the square $\text{Tl}_2\text{Ba}_2\text{CaCu}_2\text{O}_{8-\delta}$, the solid diamond $\text{La}_{2-x}\text{Sr}_x\text{PCaCu}_2\text{O}_6$, the small solid square $\text{HgBa}_2\text{Ca}_2\text{Cu}_3\text{O}_{8-\delta}$, and the large square $\text{YBa}_2\text{Cu}_4\text{O}_8$.

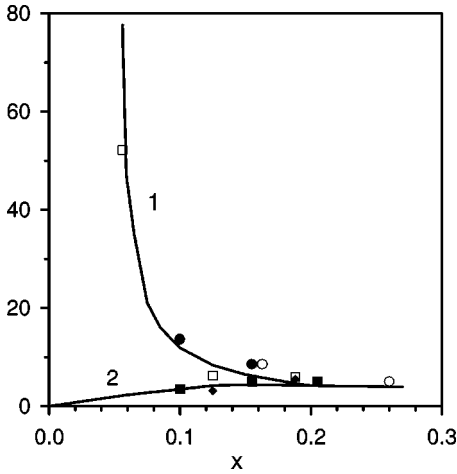


FIG. 5. The curve 1 is $2\Delta(0K)/T_c$ vs x . The circle is from Ref. 17, the solid circle Ref. 9, and the square Ref. 2. The curve 2 is $2\Delta(0K)/T^*$ vs x . The solid square is from Ref. 9, and the solid diamond Ref. 2. All the data are for B2212.

0° . At present the experimental maximum direction of PG has not yet been determined. Some experiments indicate that the maximum is at about 10° ,^{2,21-23} however, other experiments are just at 0° .^{3,4,23} It is interesting to note that Ref. 23 gave all the two maximum directions for different samples. The absence of isotope effect in PG is obvious because PG comes from TLSMI which is independent of the phonon. We guess that some high- T_c cuprates such as $\text{LaBa}_2\text{Cu}_3\text{O}_8$ have PG for overdoped samples because their Fermi surface has some variations in comparison with the nesting structure. To explain the fourteenth feature we have to know an experimental fact, i.e., the gap's values at different locations in the CuO_2 plane are different.⁵⁷⁻⁵⁹ This fact has been explained by considering that the different locations have different AF short-range coherence length, and, therefore, different values of TLSMI.⁴³ $\xi = a'/\sqrt{x} = a'/\sqrt{0.125} = 2.83a'$ is only a probable value. In fact, there are some different values of ξ in the CuO_2 plane. If $\xi = 2.83a'$, then $N''/N' = 1.325$ from the diagram of N''/N' vs ξ . Using this value, we obtain the curve 2 of Fig. 2. However, if a certain range in the CuO_2 plane has

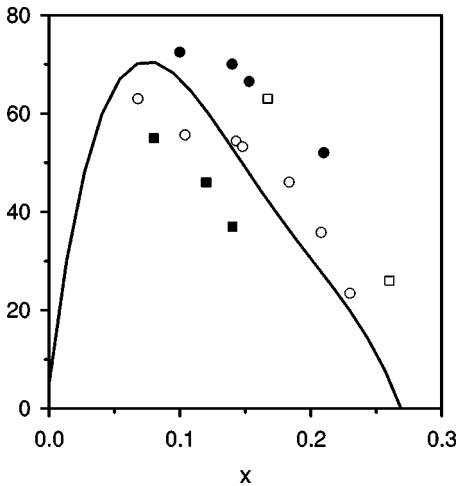


FIG. 6. Dependence of $2\Delta(0K)$ on x . The solid circle (Ref. 9), the square (Ref. 17), the solid square (Ref. 4) are for B2212, and the circle (Ref. 10) is for $\text{Y}_{0.8}\text{Ca}_{0.2}\text{BaCu}_3\text{O}_{7-\delta}$.

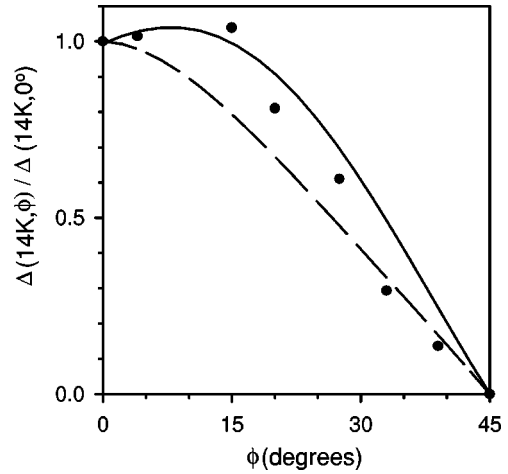


FIG. 7. Anisotropy of PG. The solid line is our theoretical composite d -wave curve for $x=0.125$. The dashed line is the simple d -wave curve in Refs. 34 and 45 for $x=0.125$. The data are for B2212 (Ref. 2).

$\xi = 6.1a'$ instead of $2.83a'$, then the curve 2 in Fig. 2 becomes the curve 1 of Fig. 8. The gap in the curve 1 of Fig. 8 has only a little change below $T_c = 83$ K. If $N''/N' = 1.4$ and $J_K = 1.1$ eV, then we obtain the curve 2 of Fig. 8 which fits the experiment in Ref. 20 better than the curve 1. The PG can exist at some locations in the CuO_2 plane of the overdoped B2212 samples because the locations can have much larger value of ξ than the probable one. Due to that we do not know the exact values of ξ, J, J_K ; the above explanation for the fourteenth feature is only a principle explanation. Here we should stress that, considering that $\xi = 2.83a'$ is the probable value, at most locations in the CuO_2 of the 83 K T_c samples used in Ref. 20 the temperature relation should be given by the curve 2 of Fig. 2 rather than the curves of Fig. 8.

V. PREDICTIONS

The curves in Fig. 3 are our predictions. In fact, the curves in Fig. 2 are also our predictions because of the large error bars. The values of the curve 1 in Fig. 2 at 50 K and 0 K are 1.006 and 1, respectively; the values of the curve 1 in

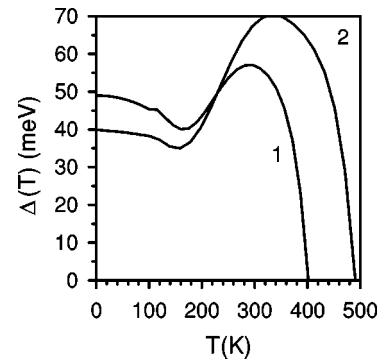


FIG. 8. Dependence of PG and the gap on T for certain chosen locations in the CuO_2 of B2212 with $x=0.125$. $\Delta(T)$ is the maximum value of our composite d -wave PG and the gap. The curve 1 is for $\xi = 6.1a'$ and $J_K = 0.78$ eV. The curve 2 is for $\xi = 3.6a'$ and $J_K = 1.1$ eV.

Fig. 3 at 50 K and 0 K are 32.65 and 32.26 meV, respectively; therefore the curves have two maximums and one minimum. Therefore, our curves in Figs. 2 and 3 show that the temperature dependences of the gap at $0 < T < T^*$ have three types, i.e., the curves with two maximums and one minimum, with one maximum, and without any extreme value. Figure 3 manifests that PG at 300 K can be 61 meV for the B2212 sample with $T_c = 0$ and $x = 0.025$.

Our theory predicts that the direction of the gap maximum value for B2212 should be at a direction about 10° rotating from the Cu-O bond, while the simple d -wave symmetry in Refs. 34, 45, and 30 just at Cu-O bond direction. At present some experiments^{2,21-23} support the former, and other experiments^{3,4,23} support the latter. The direction of the maximum gap direction is of extreme importance because the symmetry of the order parameter is determined by superconductive mechanism.

Although there is no LRPC at $T > T_c$ in the range 2 of Fig. 1, the order parameter can have short-range phase coherence. There is superconductivity in the regions being of short-range phase coherence. At present we do not know the size of the small regions being of short-range phase coherence. If the size of the small regions are much larger than the penetration depth, then a weak Meissner effect should be observed.

VI. DISCUSSIONS

It is interesting to note that our mechanism of pseudogap mainly depends on AF, therefore, in principle, our theory points out that any AF materials have the possibility of being the pseudogap. The AF materials, Fe_{1-x}S (T_c at 110 K),⁶⁰ CuCl_2 at high pressure (Meissner effect at 140 K),⁶¹ Rb_3C_{60} ,⁶² are examples. Due to the same reason our theory can also in principle explain the pseudogap in superconductive and AF quasi-2D organic systems, $(\text{ET})_2\text{X}$,^{63,64} and heavy fermion system UPt_3 .⁶⁵

APPENDIX A: EXTENDED ABRIKOSOV'S PSEUDOFERMION METHOD

In this appendix we extend Abrikosov's pseudofermion method to deal with the case of coexistence of both Kondo Hamiltonian and Heisenberg Hamiltonian, and give the obvious transformation factor.

The local spin operator \hat{S}_i at site i is represented in Abrikosov's representation as³⁵

$$\hat{S}_i = \sum_{\alpha\beta} \mathbf{S}_{\alpha\beta} d_{i\alpha}^+ d_{i\beta}, \quad (\text{A1})$$

where \mathbf{S} is spin matrix vector, and $d_{i\alpha}^+$ and $d_{i\alpha}$ are creation and annihilation operator of quasiparticle with spin α at site i . Because $d_{i\alpha}^+$ and $d_{i\alpha}$ satisfy the following anticommutation rules, the quasiparticle is called pseudo-fermion:

$$[d_{i\alpha}^+, d_{j\beta}]_+ = \delta_{ij} \delta_{\alpha\beta}, \quad (\text{A2})$$

$$[d_{i\alpha}^+, d_{j\beta}^+]_+ = [d_{i\alpha}, d_{j\beta}]_+ = 0. \quad (\text{A3})$$

Let the local spin magnitude be $\frac{1}{2}$. The pseudofermion state at site i can be written as

$$|n\rangle_i = |n \uparrow n \downarrow\rangle_i. \quad (\text{A4})$$

The \uparrow pseudofermion number $n \uparrow = 0$ or 1 , $n \downarrow = 0$ or 1 . $|01\rangle_i$ and $|10\rangle_i$ are called physical spin states. $|00\rangle_i$ and $|11\rangle_i$ are called false spin states because we deal with the spin states at site i always having one local spin with a magnitude of $\frac{1}{2}$.

The generic form of a Hamiltonian containing local spin operator is

$$H = H_0 + H_{\text{Kondo}} + H_{\text{Heisenberg}}, \quad (\text{A5})$$

$$H_0 = \sum_{\mathbf{k}\alpha} \varepsilon_{\mathbf{k}} c_{\mathbf{k}\alpha}^+ c_{\mathbf{k}\alpha}, \quad (\text{A6})$$

$$H_{\text{Kondo}} = \frac{J_K}{N_c} \sum_{i\mathbf{k}\mathbf{k}'\alpha\beta\delta\gamma} \vec{\sigma}_{\alpha\beta} \cdot \hat{S}_i c_{\mathbf{k}\alpha}^+ c_{\mathbf{k}'\beta} e^{i(\mathbf{k}-\mathbf{k}')\cdot\mathbf{R}_i}, \quad (\text{A7})$$

$$H_{\text{Heisenberg}} = J \sum_{ij} \hat{S}_i \cdot \hat{S}_j, \quad (\text{A8})$$

where H_0 is the free carrier Hamiltonian, $\varepsilon(\mathbf{k})$ the dispersion relation, $\vec{\sigma}$ the Pauli matrix vector, and N_c the cell number in a lattice. In Eq. (A8) only the nearest neighbor interaction is considered.

The statistical operators of noninteracting and interacting system are, respectively,

$$\rho_0 = e^{-(H_0 - \mu N)/T}, \quad (\text{A9})$$

$$\rho = e^{-(H - \mu N)/T}, \quad (\text{A10})$$

where μ is the chemical potential and N the carrier number operator. The full average of an operator R on both the physical and the false spin states is defined as

$$\langle R \rangle^f = \frac{\text{Tr}^f(\rho R)}{\text{Tr}^f(\rho)}, \quad (\text{A11})$$

$$\langle R \rangle_0^f = \frac{\text{Tr}^f(\rho_0 R)}{\text{Tr}^f(\rho_0)}, \quad (\text{A12})$$

$$\text{Tr}^f(\dots) = \text{Tr}_A \text{Tr}^{(1)(2)} \dots (\dots), \quad (\text{A13})$$

$$\text{Tr}_A(\dots) = \sum_{\{A\}} \langle A | \dots | A \rangle, \quad (\text{A14})$$

$$\text{Tr}^{(1)(2)} \dots (\dots) = \sum_{\{n\}} \langle n | \dots | n \rangle, \quad (\text{A15})$$

where $|A\rangle$ is the eigenstate of H_0 and $|n\rangle$ the spin eigenstate of the pseudofermion operators at all local spin sites enumerated by the numbers in the left side of Eq. (A15). Note that $|n\rangle$ contains both the physical and the false spin states

$$|n\rangle = |n\rangle_1 |n\rangle_2 \dots, \quad (\text{A16})$$

$$\begin{aligned} \text{Tr}^{(1)}(\dots) = & {}_1\langle 00 | \dots | 00 \rangle_1 + {}_1\langle 11 | \dots | 11 \rangle_1 + {}_1\langle 10 | \dots | 10 \rangle_1 \\ & + {}_1\langle 01 | \dots | 01 \rangle_1, \end{aligned} \quad (\text{A17})$$

$$\text{Tr}^{(1)'}(\dots) = {}_1\langle 01 | \dots | 01 \rangle_1 + {}_1\langle 10 | \dots | 10 \rangle_1, \quad (\text{A18})$$

$$Tr^{(1)''}(\dots) = {}_1\langle 00 | \dots | 00 \rangle_1 + {}_1\langle 11 | \dots | 11 \rangle_1, \quad (\text{A19})$$

where we use a single prime to represent the physical spin states, and a double prime the false spin states. The physical average of R , $\langle R \rangle$, should be taken on $|A\rangle$ and the physical spin states

$$\langle R \rangle = \frac{Tr(\rho R)}{Tr(\rho)}, \quad (\text{A20})$$

$$\langle R \rangle_0 = \frac{Tr(\rho_0 R)}{Tr(\rho_0)}, \quad (\text{A21})$$

$$Tr(\dots) = \sum_{\{A\}} \langle A | \sum_{\{n'\}} \langle n' | \dots | n' \rangle | A \rangle. \quad (\text{A22})$$

Because $|n'\rangle$ is only a subspace of the pseudo-fermion operator, i.e., the physical spin state, we cannot use the linked cluster expansion theorem in the calculation of $\langle R \rangle$.

In the following we show

$$\langle R \rangle - \langle R \rangle_0 = w(J/T)(\langle R \rangle^f - \langle R \rangle_0^f), \quad (\text{A23})$$

and derive the expression of $w(J/T)$. Assuming R is independent of the local spin operator, we know from definitions that $\langle R \rangle_0 = \langle R \rangle_0^f$. $\langle R \rangle$ can be rewritten as

$$\langle R \rangle = \frac{Tr(\rho R)}{Tr^f(\rho R)} \frac{Tr^f(\rho)}{Tr(\rho)} \langle R \rangle^f. \quad (\text{A24})$$

All local spin sites are equivalent. At any local spin site there is the same scattering between carrier and local spin and the same coupling between local spins. Let us choose a concrete local spin site such as 1. We study how to eliminate the effect of the false local spin states on the statistical average. The Green's function may also be regarded as the statistical average of a certain operator. From definitions we have

$$Tr^f(\rho) = Tr_A Tr^{(2)(3)} \dots Tr^{(1)''}(\rho) + Tr_A Tr^{(2)(3)} \dots Tr^{(1)'}(\rho). \quad (\text{A25})$$

Our aim is to use the pseudo-fermion representation for the local spin operator to study scattering between carrier and local spin in magnetic ordering states in the text. In magnetic ordering states single spin flip is prohibited due to the energy minimum principle. Therefore for our aim we can only consider the z component of the local spin operator in Hamiltonians in Eqs. (A7) and (A8). The operations of $\sum_{\alpha\beta} S_{\alpha\beta}^\gamma d_{i\alpha}^+ d_{i\beta}$ with $\gamma=x,y,z$ on $|00\rangle_i$ or $|11\rangle_i$ are zero, which can be verified by direct calculations. From the above considerations we can rewrite Eq. (A25) as

$$Tr^f(\rho) = Tr_A(\rho_0) 2f_1 + Tr_A(\rho'_0) f_2, \quad (\text{A26})$$

$$f_1 = Tr^{(2)(3)} \dots (e^{-JX}), \quad (\text{A27})$$

$$X = \frac{1}{T} \sum_{2 \leq i < j} S_{i\alpha\alpha}^z S_{j\beta\beta}^z d_{i\alpha}^+ d_{i\alpha} d_{j\beta}^+ d_{j\beta}, \quad (\text{A28})$$

where the double subscript means spin summation,

$$f_2 = Tr^{(2)(3)} \dots (e^{-JY}), \quad (\text{A29})$$

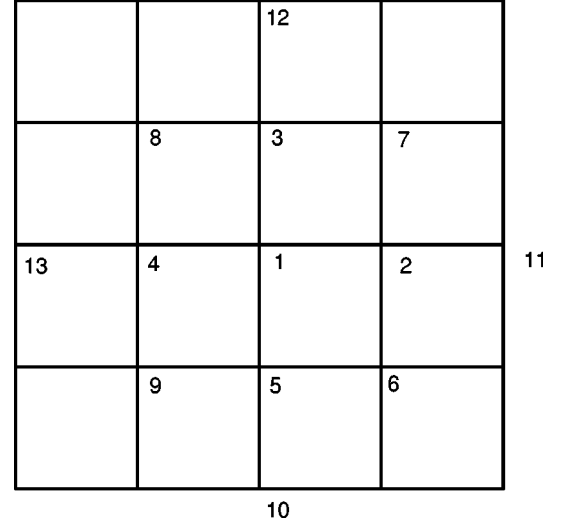


FIG. 9. A numbered square lattice. The crossing points of two lines are the sites of the local spins.

$$Y = X + \frac{1}{2T} \sum_j' S_{j\alpha\alpha}^z d_{j\alpha}^+ d_{j\alpha}, \quad (\text{A30})$$

where the prime means summation of j only over the nearest neighbors of site 1,

$$\rho'_0 = e^{-(H_0 - \mu N + E)/T} + e^{-(H_0 - \mu N - E)/T}, \quad (\text{A31})$$

$$E = \frac{J_K}{2N_c} \sum_{\mathbf{k}\mathbf{k}'} \sigma_{\alpha\alpha}^z c_{\mathbf{k}\alpha}^+ c_{\mathbf{k}'\alpha} e^{-i(\mathbf{k}-\mathbf{k}') \cdot \mathbf{R}_1}, \quad (\text{A32})$$

$$Tr(\rho) = Tr_A(\rho'_0) f_3, \quad (\text{A33})$$

$$f_3 = Tr^{(2)'}(3)' \dots (e^{-JY}). \quad (\text{A34})$$

After some basic derivations we have

$$\frac{Tr_A(\rho'_0)}{Tr_A(\rho_0)} = 2. \quad (\text{A35})$$

From Eqs. (A26), (A33), and (A35) we have

$$\frac{Tr^f(\rho)}{Tr(\rho)} = \frac{f_1 + f_2}{f_3}. \quad (\text{A36})$$

In analogy with Eqs. (A26) and (A33) we obtain

$$Tr^f(\rho R) = Tr_A(\rho_0 R) 2f_1 + Tr_A(\rho'_0 R) f_2, \quad (\text{A37})$$

$$Tr(\rho R) = Tr_A(\rho'_0 R) f_3. \quad (\text{A38})$$

From Eqs. (A37), (A26), and (A35) we have

$$\frac{Tr_A(\rho'_0 R)}{Tr_A(\rho_0)} = \frac{\langle R \rangle^f (2f_1 + 2f_2) - \langle R \rangle_0^f 2f_1}{f_2}. \quad (\text{A39})$$

From Eqs. (A37) and (A38) we have

$$\frac{Tr(\rho R)}{Tr^f(\rho R)} = \frac{f_3 \frac{Tr_A(\rho'_0 R)}{Tr_A(\rho_0)}}{2f_1 \langle R \rangle_0^f + f_2 \frac{Tr_A(\rho'_0 R)}{Tr_A(\rho_0)}}. \quad (\text{A40})$$

Substituting Eqs. (A40), (A39), and (A35) into Eq. (A24), and considering $\langle R \rangle_0^f = \langle R \rangle_0$, we have

$$\langle R \rangle - \langle R \rangle_0 = \left(1 + \frac{f_1}{f_2}\right) (\langle R \rangle^f - \langle R \rangle_0^f). \quad (\text{A41})$$

f_1 and f_2 are dependent on the distribution of local spins. We take a square lattice as an example to calculate f_1 and f_2 . Number the local spins as shown in Fig. 9. Using third neighbor approximation of site 1, and considering symmetry of the square lattice, we obtain

$$f_1 = \{Tr^{(2)(6)(7)(11)}[e^{-(J/T)[S_{2\alpha\alpha}^z d_{2\alpha}^+ d_{2\alpha} (S_{6\beta\beta}^z d_{6\beta}^+ d_{6\beta} + S_{7\beta\beta}^z d_{7\beta}^+ d_{7\beta} + S_{11\beta\beta}^z d_{11\beta}^+ d_{11\beta})}]\}^4, \quad (\text{A42})$$

$$f_2 = \{Tr^{(2)(6)(7)(11)}[e^{-(J/T)[S_{2\alpha\alpha}^z d_{2\alpha}^+ d_{2\alpha} (S_{6\beta\beta}^z d_{6\beta}^+ d_{6\beta} + S_{7\beta\beta}^z d_{7\beta}^+ d_{7\beta} + S_{11\beta\beta}^z d_{11\beta}^+ d_{11\beta}^{+1/2})}]\}^4. \quad (\text{A43})$$

Considering the definition of the trace for the pseudofermion operators in Eqs. (A15), (A16), and (A17), and completing the trace operations in Eqs. (A42) and (A43), we have

$$f_1 = [168 + 30(e^{-J/4T} + e^{J/4T}) + 12(e^{-J/2T} + e^{J/2T}) + 2(e^{-3J/4T} + e^{3J/4T})]^4, \quad (\text{A44})$$

$$f_2 = [158 + 38(e^{-J/4T} + e^{J/4T}) + 4(e^{-J/2T} + e^{J/2T}) + 6(e^{-3J/4T} + e^{3J/4T}) + e^{-J/T} + e^{J/T}]^4. \quad (\text{A45})$$

*Mailing address: Chang Chun Yuan, Building 56, Room 502, Beijing University, Beijing 100871, China. Electronic address: fslu@pku.edu.cn

¹B. G. Levi, Phys. Today **49** (6), 17 (1996).

²H. Ding, T. Yokoya, J. C. Campuzano, T. Takehaski, M. Randeria, M. R. Norman, T. Mochiku, K. Kadowaki, and J. Giapintzakis, Nature (London) **382**, 51 (1996).

³A. G. Loeser, Z.-X. Shen, D. S. Dessau, D. S. Marshall, C. H. Park, P. Fournier, and A. Kapitulnik, Science **273**, 325 (1996).

⁴J. M. Harris, Z.-X. Shen, P. J. White, D. S. Marshall, and M. C. Schebel, Phys. Rev. B **54**, 15 665 (1996).

⁵G. V. M. Williams, J. L. Tallon, E. M. Haines, R. Michalak, and R. Dupree, Phys. Rev. Lett. **78**, 721 (1997).

⁶G. V. W. Williams, J. L. Tallon, R. Michalak, and R. Dupree, Phys. Rev. B **54**, 6909 (1996).

⁷H. J. Tao, Farum Lu, and E. L. Wolf, Physica C **282-287**, 1507 (1997).

⁸M. Oda, K. Hoya, R. Kubota, C. Manabe, N. Momono, T. Nakanano, and M. Ido, Physica C **282-287**, 1499 (1997).

⁹M. Oda, K. Hoya, R. Kubota, C. Manabe, N. Momono, T. Nakanano, and M. Ido, Physica C **281**, 135 (1997).

¹⁰J. W. Loram, K. A. Mirza, J. R. Cooper, and J. L. Tallon, Physica C **282-287**, 1405 (1997).

¹¹I. Francois, J. Genoe, and G. Borghs, Phys. Rev. B **54**, 3066 (1996).

¹²A. V. Puchkov, P. Fournier, D. N. Basov, T. Timusk, A. Kapitulnik, and N. N. Kolesnikov, Phys. Rev. Lett. **77**, 3212 (1996).

¹³D. N. Basov, R. Liang, B. Dabrowski, D. A. Bonn, W. N. Hardy, and T. Timusk, Phys. Rev. Lett. **77**, 4090 (1996).

¹⁴K. Magishi, Y. Kitaoka, G.-q. Zheng, K. Asayama, T. Kondo, Y. Shimakawa, T. Manako, and Y. Kubo, Phys. Rev. B **54**, 3070 (1996).

¹⁵J. Bobroff, H. Alloul, P. Mendelk, V. Viallet, J.-F. Marucco, and D. Colson, Phys. Rev. Lett. **78**, 3757 (1997).

¹⁶H. Ding M. R. Norman, T. Yokoya, T. Takeuchi, M. Randeria, J. C. Campuzano, T. Takahashi, T. Mochiku, and K. Kadowaki,

Phys. Rev. Lett. **78**, 2628 (1997).

¹⁷C. Kendziora, R. J. Kelly, and M. Onellion, Phys. Rev. Lett. **77**, 727 (1996).

¹⁸G. V. M. Williams, J. C. Tallon, J. W. Quilty, H. J. Trodahl, and N. E. Flower, Phys. Rev. Lett. **80**, 377 (1998).

¹⁹A. Goto, H. Yasuoka, K. Otszchi, and Y. Ueda, Phys. Rev. B **55**, 12 736 (1997).

²⁰Ch. Renner, B. Revez, J.-Y. Genoud, K. Kadowaki, and O. Fischer, Phys. Rev. Lett. **80**, 149 (1998).

²¹H. Ding, M. R. Norman, J. C. Campuzano, M. Randeria, A. F. Bellman, T. Yokoya, T. Takahashi, T. Mochiku, and K. Kadowaki, Phys. Rev. B **54**, 9678 (1996).

²²J. Kane, Chen Qun, K. W. Ng, and H. J. Tao, Phys. Rev. Lett. **72**, 128 (1994).

²³Z. X. Shen and D. S. Dessau, Phys. Rep. **253**, 142 (1995).

²⁴P. A. Lee, Physica C **282-287**, 279 (1997).

²⁵Xiao-gang Wen and P. A. Lee, Phys. Rev. Lett. **76**, 503 (1996); P. A. Lee and Xiao-gang Wen, *ibid.* **78**, 4111 (1997).

²⁶H. Fukuyama, Prog. Theor. Phys. Suppl. **108**, 287 (1992).

²⁷H. Fukuyama, Physica C **282-287**, 124 (1997).

²⁸A. Sherman and M. Schreiber, Phys. Rev. B **55**, 712 (1997).

²⁹D. J. Newman and B. Ng, Phys. Rev. B **55**, 2792 (1997).

³⁰Shou-cheng Zhang, Science **275**, 1089 (1997).

³¹S. Doniach and M. Inui, Phys. Rev. B **41**, 6668 (1990).

³²V. J. Emery and S. A. Kivelson, Nature (London) **374**, 434 (1995).

³³B. K. Chakraverty and T. V. Ramakrishnan, Physica C **282-287**, 290 (1997).

³⁴D. J. Scalapino, Phys. Rep. **250**, 329 (1995).

³⁵Fu-sui Liu, Zhongcheng Wang, Wan-fang Chen, and Xiao-jian Yuan, Phys. Rev. B **51**, 12 491 (1995).

³⁶Fu-sui Liu and Ming Xiao, Phys. Lett. A **186**, 423 (1994).

³⁷Ming Xiao and Fu-sui Liu, Commun. Theor. Phys. **20**, 147 (1993).

³⁸Fu-sui Liu, Physica C **253**, 165 (1995).

³⁹Fu-sui Liu, Physica C **248**, 171 (1995).

- ⁴⁰Fu-sui Liu, Phys. Lett. A **224**, 185 (1997).
- ⁴¹Fu-sui Liu, Zhong-cheng Wang, Xiao-jian Yuan, and Wan-fang Chen, Phys. Lett. A **210**, 337 (1996).
- ⁴²Fu-sui Liu and Jing-yi Wang, Mod. Phys. Lett. B **10**, 815 (1996).
- ⁴³Fu-sui Liu and Ping Ma, Physica C **282-287**, 1643 (1997).
- ⁴⁴Fu-sui Liu and Jing-yi Wang, Physica C **280**, 61 (1997).
- ⁴⁵D. Pines and P. Monthoux, J. Phys. Chem. Solids **56**, 1651 (1995).
- ⁴⁶D. S. Dessau, Z.-X. Shen, D. M. King, D. S. Marshall, L. W. Lombardo, P. H. Dickinson, A. G. Loesser, J. DiCarlo, C.-H. Park, A. Kapitulnik, and W. E. Spicer, Phys. Rev. Lett. **71**, 2781 (1993).
- ⁴⁷M. Oda, T. Ohguro, H. Matsuki, N. Yamada, and M. Ido, Phys. Rev. B **41**, 2605 (1990).
- ⁴⁸K. B. Lyons, P. A. Fleury, L. F. Schneemeyer, and J. V. Waszczak, Phys. Rev. Lett. **60**, 732 (1988).
- ⁴⁹P. J. Birgeneau, D. R. Gabbe, H. P. Jensen, M. A. Kastner, P. J. Picone, T. R. Thurston, G. Shirane, Y. Endoh, M. Sato, K. Yamada, Y. Hidaka, M. Oda, Y. Enomoto, M. Suzuki, and T. Murakami, Phys. Rev. B **38**, 6614 (1988).
- ⁵⁰Y. Kitaoka, S. Ohsugi, K. Ishida, and K. Asayama, Physica C **170**, 189 (1990).
- ⁵¹H. Matsukawa and H. Fukuyama, J. Phys. Soc. Jpn. **58**, 2845 (1989).
- ⁵²P. Prelovsek, Phys. Lett. A **126**, 287 (1988).
- ⁵³F. C. Zhang and M. Rice, Phys. Rev. B **37**, 3759 (1988).
- ⁵⁴N. Andrei and P. Coleman, Phys. Rev. Lett. **62**, 595 (1989).
- ⁵⁵Rushan Han, C. K. Chew, K. K. Phua, and Z. Z. Gan, J. Phys.: Condens. Matter **3**, 8059 (1991).
- ⁵⁶H. Takagi, Y. Tokura, and S. Uchida, Physica C **162-164**, 1101 (1989); S. Uchida, H. Takagi, and Y. Tokura, *ibid.* **162-164**, 1677 (1989).
- ⁵⁷Jin-Xiang Liu and J. C. Goldman, Phys. Rev. Lett. **67**, 2195 (1991).
- ⁵⁸Lan-ping Wang, He Jian, and Wang Guowen, Phys. Rev. B **40**, 10 954 (1989).
- ⁵⁹E. A. Adkins and C. J. Chandler, J. Phys. C **20**, L1009 (1987).
- ⁶⁰G. A. Petrakovski, G. V. Losewa, N. I. Kuselev, S. G. Ovchenikov, N. B. Ivanova, and V. K. Chernov, Pis'ma Zh. Eksp. Teor. Fiz. **54**, 224 (1991).
- ⁶¹C. W. Chu, A. P. Rusakov, S. Huang, S. Early, T. H. Gaball, and C. Y. Huang, Phys. Rev. B **18**, 2116 (1978).
- ⁶²S. Teslic, T. Egami, and J. E. Foshcher, Phys. Rev. B **51**, 5973 (1995).
- ⁶³K. Kanoda, Physica C **282-287**, 299 (1997).
- ⁶⁴D. Jerome, in *Advances in Superconductivity*, edited by B. Deaver and J. Ruvalds (Plenum Press, New York, 1983), p. 129.
- ⁶⁵S. Donovan, A. Schwartz, and G. Gruner, Phys. Rev. Lett. **79**, 1401 (1997).